Copyright © 2006 American Scientific Publishers
All rights reserved
Printed in the United States of America

Journal of
Computational and Theoretical Nanoscience
Vol. 3, 142–147, 2006

Studies of Carbon Nanotube-Based Oscillators Using Molecular Dynamics

Shaoping Xiao,[1,*] David R. Andersen,[2] Ray P. Han,[1] and Wenyi Hou[1]

[1] Department of Mechanical and Industrial Engineering, Center for Computer-Aided Design, [2] Department of Electrical and Computer Engineering, Department of Physics and Astronomy, The University of Iowa, Iowa City, IA 52242, USA

In this study, we investigate some oscillation mechanisms of double-walled carbon nanotube-based oscillators using molecular dynamics. If an oscillator is an isolated system, stable oscillations of the inner tube inside of the outer tube can be observed with oscillatory frequencies as high as 72 GHz. If the same inner tube is used in designing nano-oscillators, molecular dynamics simulations illustrate that the length of the outer tube is the only consideration necessary for achieving various oscillatory frequencies. We also study the interlayer friction between the outer tube and the inner tube when nano-oscillators are at finite temperatures. A larger interlayer friction is observed in an oscillator when it is at a higher temperature, and the oscillation will stop quickly. The interlayer friction is also related to the chirality and defects in the outer tube. Based on the above studies, we propose to design a nanoelectromechanical oscillator system, which can provide stable oscillation.

Keywords: Nanotube, Oscillator, Nanoelectromechanical System.

1. INTRODUCTION

Since being discovered by Ijimma[1] in 1990, carbon nanotubes hold promise in designing novel nanoscale materials and devices due to carbon nanotubes' unique mechanical and electronic properties.[2] Carbon nanotubes have a high elastic modulus (~1 TPa),[3] high strength (~100 GPa), and low density so they can be used as ideal fibers in nanocomposites.[4] They can also be designed as scanning probes tips, field emission sources or used as other nanoelectronics components, such as molecular wires and diodes. As well, Bachtold and his co-workers[5] demonstrated logic circuits with field-effect transistors based on individual carbon nanotubes. Kinaret et al.[6] investigated the operational characteristics of a nanorelay in which a conducting carbon nanotube was placed on a terrace in a silicon substrate. Other carbon nanotube-based devices and machines include nanotweezers,[7] nanogears,[8] a nanocantilever device[9] and a nanotube motor.[10]

A multi-walled carbon nanotube (MWNT) consists of a number of co-axial single-walled nanotubes (SWNT). Cumings and Zettl[11] realized the ultra-low friction between nanotube walls in nanoscale linear bearings and constant-force nanosprings when demonstrating the controlled and reversible telescopic extension of multi-walled carbon nanotubes. Consequently, MWNTs have been used to design novel nanoscale devices based on the relative motion of nanotube walls. Lozovik et al.[12] proposed the use of double-walled nanotubes as nut and bolt pairs since they found that the relative motion of nanotube walls was controlled by the potential relief of interlayer interaction energy. A nanoswitch[13] was designed with the assumption that the corrugation of interlayer energy has no significant effects on relative motion between nanotube walls. Nanotube-based oscillators have been of interest to scientists and engineers since Zheng et al.[14,15] designed multi-walled carbon nanotubes as gigahertz oscillators in 2002. A simple nanotube-based oscillator consists of an inner tube (core) and an outer tube (shell). When the outer tube is fixed, the inner tube can oscillate inside of the outer tube once it is given an initial velocity or an initial extrusion length. The oscillatory frequency may be up to 87 GHz based on molecular dynamics simulations.[16,17] Legoas and his co-workers[17] also pointed out that stable oscillators are only possible when the interlayer distances between the outer and inner tubes are of ~0.34 nm, which equals the interlayer distance of regular MWNTs. Unlike other nanotube-based machines, energy dissipation plays a key role and needs to be considered when designing a stable nano-oscillator. Tangney et al.[18] studied mechanical energy dissipation in carbon nanotube-based oscillators and found that the interlayer friction strongly depends on the relative velocity of the tubes. In addition, the morphology combination of the tubes was found to have a significant effect on the interlayer friction.[19,20] Since nanotube-based

*Author to whom correspondence should be addressed.

1546-198X/2006/3/142/006 doi:10.1166/jctn.2006.013

oscillators are expected to have potential applications, it is crucial to design stable nano-oscillators.

In this paper, we will use molecular dynamics to investigate oscillation mechanisms of double-walled carbon nanotube-based oscillators. The computational model and methodology are described in the next section. In Section 3, we discuss effects of the outer tube, including its length and chirality, on oscillation mechanisms of nano-oscillators in which the same inner tube is used. Temperature-related interlayer friction in nano-oscillators is discussed in Section 4. Based on the simulation results, we will propose a stable nano-oscillator device design for practical applications in Section 5 followed by the conclusions.

2. COMPUTATIONAL MODEL AND METHODOLOGY

We mainly study double-walled carbon nanotube-based oscillators in this paper. A schematic representation of a [10, 10]/[5, 5] carbon nanotube-based oscillator is illustrated in Figure 1. A middle segment of the outer tube is fixed in this nanomechanical system. In this paper, the reactive empirical bond order (REBO) potential function[21] is used for describing carbon–carbon interatomic interactions in molecular dynamics simulations. This potential function considers chemical reactions and includes remote effects caused by conjugated bonding. The potential function can be written as follows:

$$E = \sum_i \sum_{j(>i)} [V^R(r_{ij}) - b_{ij} V^A(r_{ij})] \quad (1)$$

where r_{ij} is the bond length, $V^R(r)$ and $V^A(r)$ are pair-additive interactions that represent all interatomic repulsions and attractions from valence electrons, respectively. b_{ij} contains the functions that depend on the local coordinates and bond angles for atoms i and j. The detailed formulations of REBO can be found in Ref. [21]. The equilibrium carbon–carbon bond length obtained by minimizing this potential is 0.142 nm. The REBO potential function has been widely used to investigate mechanical properties of carbon nanostructures, such as diamond, graphene sheets, and carbon nanotubes. The calculated properties agree with the experimental results.

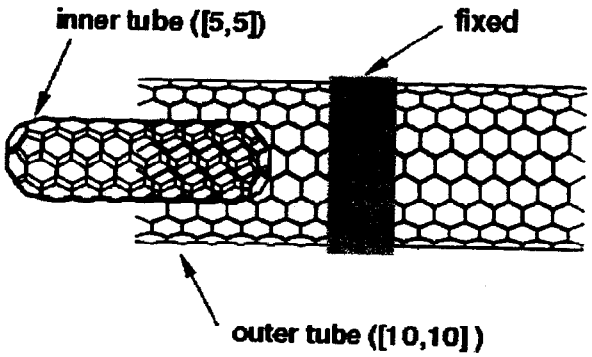

Fig. 1. A [10, 10]/[5, 5] carbon nanotube-based oscillator.

In addition, the following Lennard-Jones 6-12 potential[22] will be used as the van der Waals energy for interlayer interactions between the outer tube and the inner tube.

$$E_{LJ}(r) = A\left[\frac{1}{2}\frac{y_0^6}{r^{12}} - \frac{1}{r^6}\right] \quad (2)$$

where $A = 2.43 \times 10^{-24}$ J nm^6 and $y_0 = 0.3834$ nm. Minimizing the Lennard-Jones potential results in an equilibrium interlayer distance of 0.34 nm, which equals the thickness of a graphene sheet. Consequently, in molecular dynamics simulations, the equations of motion can be written as follows for two-walled carbon nanotube-based oscillators, based on classical Lagrangian or Hamiltonian mechanics, if there is not any external force:

$$m_I \ddot{\mathbf{d}}_I = -\frac{\partial(E_{inner} + E_{outer} + E_{LJ})}{\partial \mathbf{d}_I} \quad (3)$$

where E_{inner} and E_{outer} are potentials of the inner tube and the outer tube, respectively, as calculated from Eq. (1), m_I is the mass of atom I and $\mathbf{d}_I$ is its displacement.

Before performing molecular dynamics simulations, we conduct the energy minimization for the double-walled carbon nanotube. As a result, the inner tube is inside of the outer tube, and they have a common axis. The initial condition for the simulations corresponds to positioning the inner tube with an initial extrusion length as shown in Figure 1. The simulation starts once the inner tube is released without initial velocity. The initial temperature of the oscillator system is assumed to be 0 K. In this paper, we always consider an [5, 5] inner tube with the length of $L_{inner} = 2.5$ nm.

3. EFFECTS OF THE OUTER TUBE

We first investigate the oscillation mechanism of an isolated [10, 10]/[5, 5] nanotube-based oscillator, i.e. no heat exchange between the oscillator and its surrounding. The length of the [10, 10] outer tube is $L_{outer} = 3.7$ nm. Since the initial extrusion length is half of the inner tube length, the initial separation distance between the centers of the inner and outer tubes is half of the outer tube length. When the inner tube is released without any initial velocity, the interlayer force, due to the van der Waals energy between the inner tube and the outer tube, will drive the inner tube to move towards the center of the outer tube. The center-of-mass velocity of the inner tube reaches its maximum value after it travels a so-called accelerating distance, L_{accl}. At that point, the interlayer potential is the minimum. After the inner tube passes the center of the outer tube, the center-of-mass velocity of the inner tube starts to decrease when the interlayer potential increases. Once the center-of-mass velocity of the inner tube becomes zero, the separation distance reaches the maximum magnitude, and the interlayer potential is the maximum. Then, the interlayer force tends

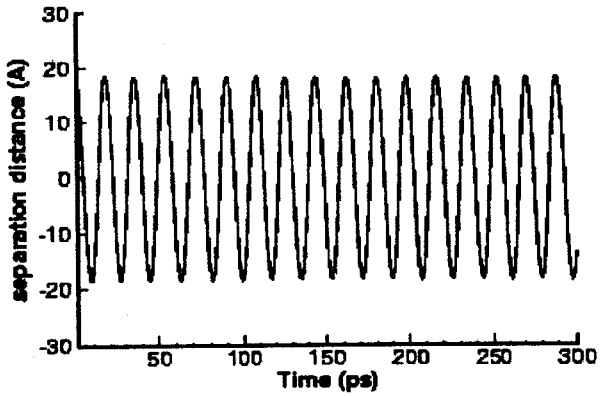

Fig. 2. Profile of center-of-distance separation between the inner tube and the outer tube.

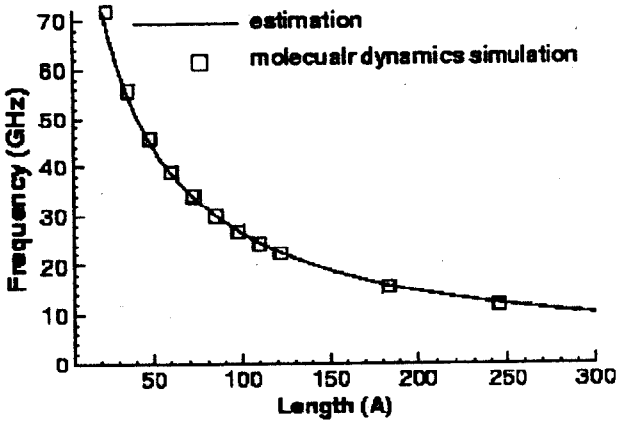

Fig. 3. The relationship between the nano-oscillator frequency and the length of the outer tube.

to drive the inner tube backwards to the center of the outer tube.

The profile of separation distance between the inner tube and the outer tube is shown in Figure 2 during the oscillation of the inner tube inside of the outer tube. We can see that the amplitude of the separation distance keeps constant, and it is equal to the initial extrusion length. As a conclusion, the oscillation of this nanomechanical oscillator is stable and the calculated oscillatory frequency is 55.55 GHz, which is referred to as the reference oscillatory frequency of this nano-oscillator. If larger extrusion lengths are used, a rocking motion[23,24] is observed at the beginning of the oscillation. The amplitude of separation distance will decay to a constant, and a similar oscillatory frequency can be obtained. In the following simulations, we only consider the extrusion length to be half of the inner tube length, $L_{extru} = 1.25$ nm.

We first employ [10, 10] carbon nanotubes with various lengths as the outer tube to study its length effects on the oscillation mechanism of [10, 10]/[5, 5] nanotube-based oscillators. From Figure 2, the accelerating distance can be estimated as $L_{accl} = 0.6$ nm, through which the center-of-mass velocity of the inner tube increases from zero to a constant. The maximum center-of-mass velocity can also be calculated from Figure 2 and is about $V_0 = 660$ m/s. Obviously, the accelerating distance and the maximum center-of-mass velocity are related to the initial extrusion length and the inner tube length. They are constants because the initial extrusion length and the inner tube length are fixed in this paper. For simplification, we assume the mean interlayer force applied on the inner tube linearly decreases to zero when the inner tube travels through the accelerating distance so that the elapsed time can be approximately by $t_1 = 3L_{accl}/V_0$. Therefore, the oscillatory frequency can be estimated once the length of the outer tube is given through the following formula:

$$f = \frac{1}{2(2t_1 + \frac{L_{outer} - 2L_{accl}}{V_0})} = \frac{2V_0}{(L_{outer} + 4L_{accl})} \quad (4)$$

Figure 3 illustrates the effect of the length of the outer tube on the nano-oscillator frequency. The oscillatory frequency can be as high as 72 GHz when length of the outer tube equals that of the inner tube. Figure 3 also shows that Eq. (4) can accurately predict oscillatory frequencies since they agree with the results from molecular dynamics simulations.

In the above studies, both the outer tube and the inner tube have the same chirality (armchair). Here, we study the oscillation mechanisms of nano-oscillators in which the outer tube and the inner tube have different chiralities. Since the inner tube is kept as a capped [5, 5] armchair nanotube, outer tubes with various chiralities are studied here. Leogas et al.[17] stated that the interlayer distance between the outer tube and the inner tube of a stable nano-oscillator should be around 0.34 nm. Therefore, we maintain the interlayer distance in a range of 0.32 nm to 0.35 nm for all the simulated double-walled carbon nanotubes in this study as listed in Table I. Lengths of the outer tubes are chosen around 3.62 nm to compare the reference oscillatory frequency that we obtained for the [10, 10]/[5, 5] nanotube-based oscillator in the above study. All the calculated frequencies are around 56 GHz, as shown in Table I. We can see that chirality of the outer tube does not significantly affect the calculated oscillatory frequency once the length of the outer tube is defined.

Table I. Comparison of oscillatory frequencies of nano-oscillators that have different chirality combinations.

Nano-Oscillators	Interlayer distance (nm)	Length of the outer tube (nm)	Calculated frequency (GHz)
[17,0]/[5,5]	0.326	3.55	55.25
[16,2]/[5,5]	0.33	3.67	56.18
[15,4]/[5,5]	0.34	3.61	56.82
[14,5]/[5,5]	0.329	3.68	54.05
[13,7]/[5,5]	0.349	3.57	56.18
[12,8]/[5,5]	0.344	3.60	57.47
[10,10]/[5,5]	0.339	3.62	55.55
Mean value	0.336714	3.614286	55.92857
Standard deviation	0.007923	0.044355	1.030249

4. TEMPERATURE EFFECTS

Guo et al. has investigated temperature effects on energy dissipation in gigahertz nanotube oscillators.[20] In their studies, if an initial finite temperature was given in an isolated nano-oscillator, the system energy would be dissipated. Based on the above studies in Section 3, we found that an isolated nano-oscillator would be stable if the initial temperature equals zero. However, this is a very rare situation. In this paper, we also investigate the temperature effects on oscillation mechanisms of the [10, 10]/[5, 5] carbon nanotube-based oscillator. Here, the outer tube has the length of 3.62 nm. As a difference with,[20] the outer tube is assumed to have heat transfer with its surrounding to model the practical usages of the nano-oscillators. A Hoover thermostat[25] is implemented so that the temperature of the outer tube can be maintained as a constant. We first study the oscillation mechanism of the nano-oscillator at 300 K. As shown in Figure 4, we find that a stable oscillatory frequency and amplitude cannot be obtained. The oscillatory amplitude decays until the nano-oscillator eventually stops. This phenomenon is caused by interlayer friction, which mainly dissipates the interlayer energy of the oscillator. Such dissipated energy was transferred to kinetic energy of the outer tube, and the artificial thermostat thereafter dissipates the energy of the outer tube. Consequently, the whole energy of the system is dissipated.

To study the temperature-related interlayer friction, three different temperatures are considered: 100 K, 300 K, and 1000 K. Figure 5 shows the evolutions of the maximum interlayer energy of the nano-oscillator when the outer tube is at various temperatures. It can be seen that a nano-oscillator dissipates energy faster at a higher temperature. We calculate the effective interlayer friction at 0.05 ns based on the following equation:[19]

$$F_{\text{eff}} = \frac{1}{4\xi_{\max} f} \frac{dE_{\text{LJ}}}{dt} \tag{5}$$

where $\xi_{\max}$ is the oscillatory amplitude of the nanotube-based oscillator, f the oscillatory frequency, and dE_{LJ}/dt

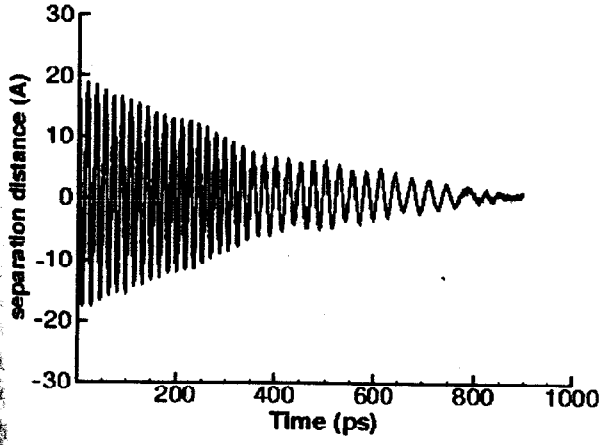

Fig. 4. Oscillating of the oscillator at 300 K.

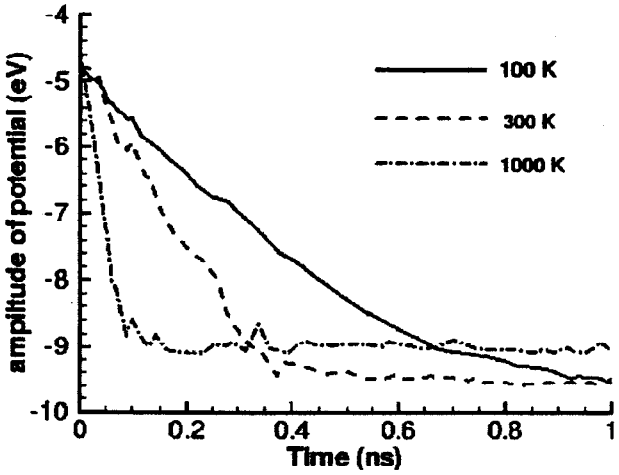

Fig. 5. Interlayer energy dissipation at different temperatures.

the interlayer energy dissipation rate. Here, we think the interlayer friction results in the energy dissipation, mainly the interlayer energy dissipation. The calculated effective frictions are 0.0021, 0.0053, and 0.0133 pN per atom for the oscillator at temperatures of 100 K, 300 K, and 1000 K, respectively. The interlayer friction is in the same order of what Cumming and Zettles[11] predicted, i.e. 0.015 pN per atom. Our studies show that the interlayer friction will be larger under a higher temperature. We can see that the oscillator will stop in a very short time, i.e. 0.1 ns, at a temperature of 1000 K.

Only pristine nanotubes are considered in the above studies. However, defects can exist in carbon nanotubes. Those defects include: (a) chemical defects consisting of atoms/groups covalently attached to the carbon lattice of the tubes; (b) topological defects corresponding to the presence of rings other than hexagons; and (c) vacancy defects due to impact by high energy electrons in the transmission electron microscope (TEM) environment or holes in the original outer nanotube shell. Here, we mainly consider [10, 10] outer tubes with vacancy defects, and the [5, 5] inner tube is assumed to be pristine. Only one-atom

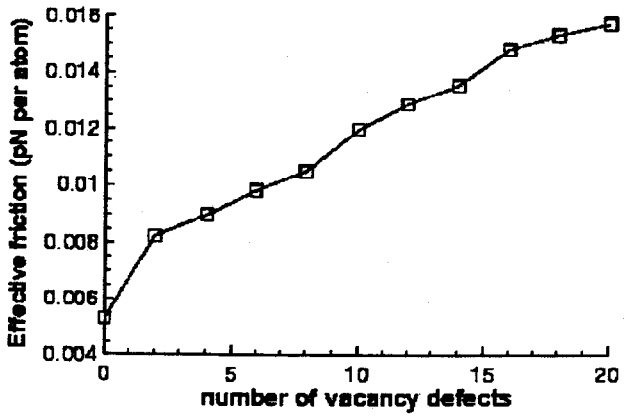

Fig. 6. Effective interlayer friction related to the number of vacancy defects.

Table II. Comparison of interlayer friction when nano-oscillators are at a temperature of 300 K.

Nano-oscillators	[10,10]/[5,5]	[13,7]/[5,5]	[15,4]/[5,5]	[12,8]/[5,5]	[17,0]/[5,5]	[16,2]/[5,5]	[14,5]/[5,5]
Interlayer friction (pN per atom)	0.0053	0.0060	0.0065	0.0072	0.0096	0.0144	0.0153

vacancy defects are considered in the outer tube here. Such a defect is produced by taking out one atom randomly and then reconstructing bonds.[26] We investigate the effects of the number of vacancy defects on the effective interlayer friction when the [10, 10]/[5, 5] nano-oscillator is at 300 K. Up to twenty one-atom vacancy defects are considered. For any specific number of vacancy defects, several simulations are performed since the locations of vacancies are randomly generated. The average effective interlayer friction is illustrated in Figure 6. Figure 6 shows that a larger number of vacancy defects result in larger interlayer friction.

In Section 3, we concluded that the chirality of the outer tube has no significant effect on reference oscillatory frequency of nano-oscillators with the same inner tube. Here, we study nano-oscillators as listed in Table I but at a temperature of 300 K. The calculated interlayer frictions at 0.1 ns are listed in Table II. We can see that the chirality of the outer tube has significant effects on the interlayer friction. For nano-oscillators with an armchair inner tube, an armchair outer tube results in the smallest interlayer friction when compared with other outer tubes with different chiralities. Guo et al.[20] also pointed out that the interlayer friction in a zigzag/armchair nano-oscillator is larger than the one in an armchair/armchair nano-oscillator. Table II also showed that the interlayer friction has a large variation and it can be as large as 0.0153 pN per atom when a [14, 5] nanotube is used as the outer tube in the nano-oscillator.

5. A NANOTUBE-BASED NANOELECTROMECHANICAL OSCILLATOR

The above simulations result in a conclusion that a stable nanotube-based oscillator should be isolated with an initial zero temperature. This requirement would limit the applications of nano-oscillators since a stable nano-oscillator at specific temperatures, especially high temperatures, is attractive to engineers. Here, we propose to design a stable nanoelectromechanical oscillator as shown in Figure 7. In the proposed design, the two-walled carbon nanotube is positioned on the top of a conducting groundplane. Atomic materials for the conducting electrodes 1 and 2 are deposited on the top of the outer nanotube. In this configuration the inner tube sits in a double-bottom electromagnetic potential well. The depth of the potential well under electrode 1 is proportional to the voltage applied to electrode 1, and similarly, the depth of the potential well under

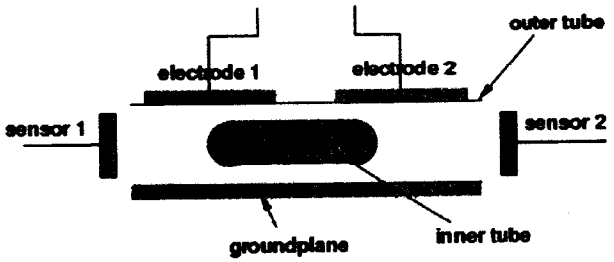

Fig. 7. A nanoelectromechanical oscillator.

electrode 2 is proportional to the voltage applied to electrode 2. Assuming a voltage V is applied to the electrode and recalling that the energy stored in a capacitor is $W = CV^2/2$, where C represents the capacitance of the system as a function of inner nanotube position, the axial electromagnetic forces, f^{el}, acting on atoms of the inner nanotube, can be written:

$$f^{el}(z) = \frac{\partial W}{\partial z}\bigg|_V = \frac{1}{2}V^2\frac{\partial C}{\partial z} \tag{6}$$

where z is the axial position of the atom in the inner tube. Such electromagnetic force is in the direction of the higher electric field density, and therefore serves to localize the inner nanotube underneath the electrode with the higher applied voltage. Equation (3) can thereafter be rewritten as:

$$m_I\ddot{\mathbf{d}}_I = f^{el} - \frac{\partial\phi}{\partial\mathbf{d}_I} \tag{7}$$

Two sensors are placed on the ends of nanotube. They have the following functions: (1) preventing the inner tube from escaping the outer tube due to electromagnetic forces; (2) generating the signal when the inner tube reaches the sensor and produces pressure on the sensor. Such signals will be read as switchable logical 1/0. In this nanoelectromechanical oscillator, the inner tube may be induced to move by applying a high voltage to the electrode opposite the position of the inner nanotube while another electrode is applied with a low voltage. If the electromagnetic force due to the applied high voltage is sufficiently strong, the static friction acting upon the inner nanotube may be overcome and lateral motion will be induced as a result. For example, when a high voltage is applied to electrode 1 and a low voltage is applied to electrode 2, the inner tube will move to lie underneath electrode 1 due to the force induced by the inhomogeneous electromagnetic field inside the outer tube. A signal was generated at sensor 1 when it was pressured by the inner tube. This signal can be read as logical 1. Then, if a high voltage is applied on electrode 2 and a low voltage is applied on electrode 1, the inner tube will move from left to right due to the induced electromagnetic forces. Consequently, the inner tube can move to reach sensor 2, which will generate a logical 0 signal.

It should be noted that the outer tube should be metallic and the inner tube can be semiconductor or metallic. As an example, we employ a [10, 10]/[5, 5] nanotube in Table I in the proposed nanoelectromechanical oscillator since all

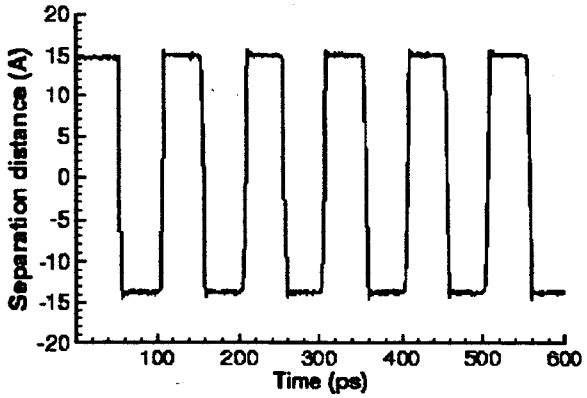

(a) frequency of 10 GHz

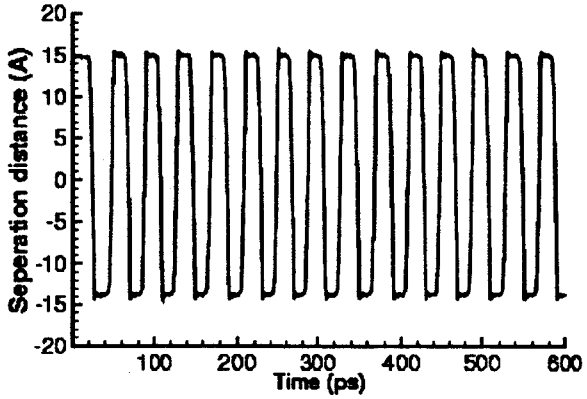

(b) frequency of 25 GHz

Fig. 8. Oscillating of a [10,10]/[5,5] double-walled nanotube-based nanoelectromechanical oscillator when electrodes are applied in different voltage pulses.

the armchair carbon nanotubes are metallic. The reference oscillatory frequency of the nano-oscillator is 55 GHz. It is no doubt that a nanoelectromechanical oscillator cannot have the frequency that exceeds its reference oscillatory frequency. Indeed, the frequency relies on the frequency of the voltage pulse applied on the electrodes as shown in Figure 8.

6. CONCLUSIONS

Molecular dynamics is used to investigate oscillation mechanisms of double-walled carbon nanotube-based oscillators. If the oscillator system is an isolated system with an initial temperature of 0 K, a stable oscillation can be observed. The studies show that the oscillatory frequency depends on the length of the outer tube but not the chirality of the outer tube if the same inner tube is employed. We also found that a nano-oscillator would stop if there were heat exchanges between it and its surroundings. The interlayer friction could be larger with a higher temperature. It also has been shown that defects on the outer tube and its chirality have significant effects on the temperature-related interlayer friction. If a [10, 10]/[5, 5] nanotube-based oscillator was under a room temperature, it would stop in 2 nanoseconds. Such a phenomenon blocks the nanotube-based oscillators from being used in engineering applications. A design for nanoelectromechanical oscillators with stable frequencies was proposed in this paper. This nanoelectromechanical system was designed by coating electrodes on the outer tube so that the induced electromagnetic forces can overcome the temperature-related interlayer friction. The frequency of such an oscillator depends on the frequency of voltage pulses applied on the electrodes.

Acknowledgments: Xiao and Hou acknowledge startup fund supports from the College of Engineering and the Center for Computer-Aided Design (CCAD) at the University of Iowa. Andersen acknowledges support from NIH Grant No. DK64659.

References

1. S. Iijima, *Nature* 354, 56 (**1991**).
2. V. N. Popov, *Mater. Sci. Eng. R* 43, 61 (**2004**).
3. T. Belytschko, S. P. Xiao, G. C. Schatz, and R. S. Ruoff, *Phys. Rev. B* 65, 235430 (**2002**).
4. A. B. Dalton, S. Collins, J. Razal, E. Munoz, V. H. Ebron, B. G. Kim, J. N. Coleman, J. P. Ferraris, and R. H. Baughman, *J. Mater. Chem.* 14, 1 (**2004**).
5. A. Bachtold, P. Hadley, T. Nakanishi, and C. Dekker, *Science* 294, 1371 (**2001**).
6. J. M. Kinaret, T. Nord, and S. Viefers, *Appl. Phys. Lett.* 82, 1287 (**2003**).
7. P. Kim and C. M. Lieber, *Science* 286, 2148 (**1999**).
8. D. Srivastava, *Nanotechnology* 8, 186 (**1997**).
9. C. Ke and H. D. Espinosa, *Appl. Phys. Lett.* 85, 681 (**2004**).
10. J. W. Kang and H. J. Hwang, *Nanotechnology* 15, 1633 (**2004**).
11. J. Cumings and A. Zettl, *Science* 289, 602 (**2000**).
12. Y. E. Lozovik, A. V. Minogin, and A. M. Popov, *Phys. Lett. A* 313, 112 (**2003**).
13. L. Forro, *Science* 289, 560 (**2000**).
14. Q. S. Zheng and Q. Jiang, *Phys. Rev. Lett.* 88, 045503 (**2002**).
15. Q. S. Zheng, J. Z. Liu, and Q. Jiang, *Phys. Rev. B* 65, 245409 (**2002**).
16. S. B. Legoas, V. R. Coluci, S. F. Braga, P. Z. Coura, S. O. Dantas, and D. S. Galvao, *Phys. Rev. Lett.* 90, 055504 (**2003**).
17. S. B. Legoas, V. R. Coluci, S. F. Braga, P. Z. Coura, S. O. Dantas, and D. S. Galvao, *Nanotechnology* 15, S184 (**2004**).
18. P. Tangney, S. G. Louie, and M. L. Cohen, *Phys. Rev. Lett.* 93, 065503 (**2004**).
19. J. L. Rivera, C. McCabe, and P. T. Cummings, *Nanotechnology* 16, 186 (**2005**).
20. W. L. Guo, Y. F. Guo, H. J. Gao, Q. S. Zheng, and W. Y. Zhong, *Phys. Rev. Lett.* 91, 125501 (**2003**).
21. D. W. Brenner, O. A. Shenderova, J. A. Harrison, S. J. Stuart, B. Ni, and S. B. Sinnott, *J. Phys.: Condens. Matter* 14, 783 (**2002**).
22. C. A. Girifalco and R. A. Lad, *J. Chem. Phys.* 25, 693 (**1956**).
23. Y. Zhao, C. C. Ma, G. H. Chen, and Q. Jiang, *Phys. Rev. Lett.* 91, 175504 (**2003**).
24. S. P. Xiao, R. Han, and W. Y. Hou, *Int. J. Nanosci.* (**2005**), submitted.
25. W. G. Hoover, *Phys. Rev. A* 31, 1695 (**1985**).
26. S. L. Mielke, D. Troya, S. L. Zhang, J. L. Li, S. P. Xiao, R. Car, R. S. Ruoff, G. C. Schatz, and T. Belytschko, *Chem. Phys. Lett.* 390, 413 (**2004**).

Received: 8 July 2005. Accepted: 24 August 2005.